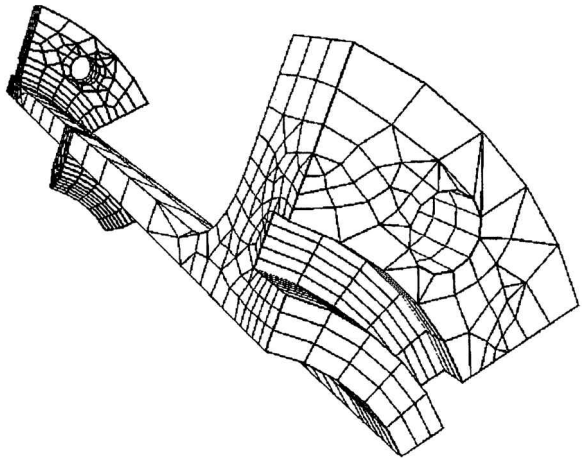

a) Surface mesh: original

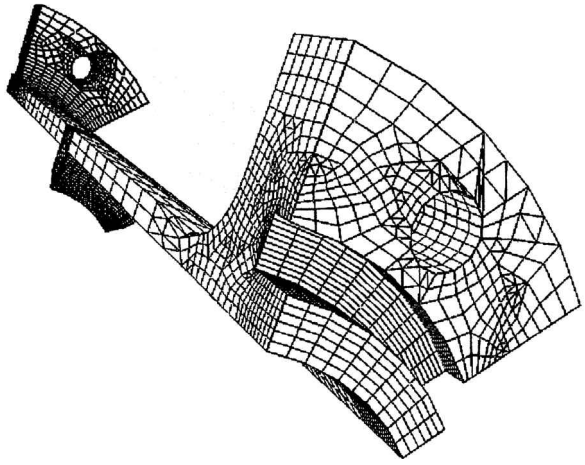

b) Surface mesh: h refined

Fig. 4 Existing finite element mesh h refinement.

Conclusions

Methodology and computer software have been developed and assembled into a generalized meshing environment for computational mechanics. It was shown that the generalized tools can generate unstructured meshes from commercial CAD databases, repair/improve existing meshes, and locally remesh/refine meshes from commercial finite element codes. The conclusion is then reached that this meshing environment is a very general tool with extensive and valuable applications to computational mechanics and is a step forward in advancing the critical automation of meshing technology.

Acknowledgment

This work was sponsored in part through Small Business Innovation Research contracts with NASA: NASA Marshall Space Flight Center Contract NAS8-40164.

References

[1]Thompson, J. F., and Weatherill, N. P., "Aspects of Numerical Mesh Generation: Current Science and Art," AIAA Paper 93-3539, June 1993.

[2]Löhner, R., and Parikh, P., "Three-Dimensional Mesh Generation by the Advancing Front Method," *International Journal for Numerical Methods in Fluids*, Vol. 8, July 1989, pp. 1135–1149.

[3]Spradley, L.W., and Anderson, P. G., "Finite Difference Mesh Generation by Multivariate Blending Function Interpolation," NASA CP-2166, Oct. 1980.

[4]Thompson, J. F., "Composite Grid Generation Code for General Three-Dimensional Regions, The Eagle Code," *AIAA Journal*, Vol. 26, No. 3, 1988, pp. 271, 272.

[5]Mavriplis, D. J., "An Advancing Front Delaunay Triangulation Algorithm Designed for Robustness," AIAA Paper 93-0671, Jan. 1993.

[6]McMorris, H., and Kallinderis, Y., "Octree-Advancing Front Method for Generation of Unstructured Surface and Volume Meshes," *AIAA Journal*, Vol. 35, No. 6, 1997, pp. 976–984.

[7]Blacker, T. D., and Stephenson, M. B., "Paving: A New Approach to Automatic Quadrilateral Mesh Generation," *International Journal for Numerical Methods in Engineering*, Vol. 32, May 1991, pp. 811–847.

[8]Cabello, J., Löhner, R., and Jacquotte, O. P., "A Variational Method for the Optimization of Two- and Three-Dimensional Unstructured Meshes," AIAA Paper 92-0450, Jan. 1992.

[9]Spradley, L. W., Löhner, R., and Mahaffey, W. A., III, "Mesh Optimization Tools for Complex Structural Models," ResearchSouth, Inc., Final Rept., NAS8-40164, Huntsville, AL, Jan. 1996.

[10]"ANSYS, Version 4.4a, Version 5.0," ANSYS Corp., Houston, PA, March 1994.

[11]"Intergraph Finite Element Modeling Packages, I/FEM and I/FEMp," Intergraph Corp., Huntsville, AL, Nov. 1993.

[12]"PATRAN Software," PDA Corp., Los Angeles, CA, March 1993.

[13]"MSC/NASTRAN User's Manual," Vol. 1, Version 67, McNeal–Schwendler Corp., Los Angeles, CA, Oct. 1991.

[14]Whirley, R. C., and Hallquist, J. O., "DYNA3D—A Nonlinear Explicit, Three Dimensional Finite Element Code for Solid and Structural Mechanics—User's Manual," Lawrence Livermore National Labs., UCRL-MA 107254, rev. 1, Livermore, CA, March 1993.

J. Kallinderis
Associate Editor

Jets in Ground Effect with a Crossflow

Jorge M. M. Barata*
Universidade da Beira Interior, 6200 Covilhã, Portugal

Nomenclature

D	= diameter of the jet
H	= height of crossflow channel
k	= turbulent kinetic energy
p	= pressure
Re	= Reynolds number
U	= horizontal velocity, $\bar{U} + u'$
$\bar{U}, \bar{V}$	= mean velocities
u', v'	= fluctuating velocities
V	= vertical velocity, $\bar{V} + v'$
X	= horizontal coordinate (positive in the direction of crossflow)
Y	= vertical coordinate (positive in the direction of jet flow)
Z	= transverse coordinate (positive on the right side of the crossflow duct looking upstream)
ε	= dissipation rate of k

Subscripts

j	= jet exit
0	= crossflow

Introduction

TURBULENT jets impinging on flat surfaces through a low-velocity crossflow are typical in impingement cooling applications in industry, as well as in the flow beneath a short/vertical takeoff aircraft that is lifting off or landing with zero or small forward momentum. In this latter application the lift jets interact strongly with the ground plane, resulting in lift losses, enhanced entrainment close to the ground (suckdown), engine thrust losses following reingestion of the exhaust gases, and possible aerodynamic instabilities caused by fountain impingement on the aircraft underside.

Received Dec. 9, 1996; presented as Paper 97-0715 at the AIAA 35th Aerospace Sciences Meeting, Reno, NV, Jan. 6–9, 1997; revision received May 28, 1998; accepted for publication June 9, 1998.

*Associate Professor, Aeronautical Sciences Department, Rua Marquês d'Ávila e Bolama. Member AIAA.

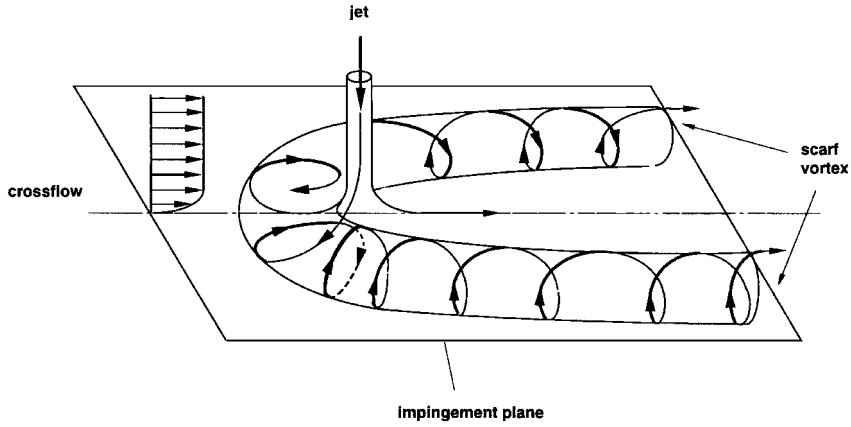

Fig. 1 Sketch of flow development for a jet impinging on a flat surface through a low-velocity crossflow.

The present results include estimates of the convection and production terms involved in the budget of turbulent kinetic energy based on the laser Doppler velocimetry measurements of Barata et al.[1] The purpose is to assess the importance of extra source terms derived from the large flow distortion in the impinging zone and to examine the implications for calculation schemes.

The present analysis explains in detail the reasons for the failure of the $k-\varepsilon$ turbulence model to predict the structure of the impinging zone and the location of the ground vortex reported by Barata et al.[1] In particular, large overpredictions of the Reynolds shear stresses in the impinging zone and significant regions where the sign is wrong were detected. Nevertheless, good predictions of the mean flow were obtained. This surprising behavior of the computational method is clearly explained in the next section.

Results and Discussion

Measurements of the velocity characteristics of normal impinging jets on a flat plate have been reported using either probe or optical techniques as reviewed, for example, by Barata et al.[1] Before the detailed measurements, the visualization studies of Barata et al.[1] have identified the formation of an impingement region characterized by considerable deflection of the impinging jet. The flow becomes almost parallel to the ground plate, and a recirculating flow region far upstream of the impinging jet is formed due to the interaction of the backward wall jet with the crossflow. The result is the formation of a ground vortex wrapped around the impinging jet in the way shown in the sketch of Fig. 1, which resembles the horseshoe vortex structure known to be generated by the deflection of a boundary layer by a solid obstacle; for example, see Ref. 2.

Errors incurred in the measurements are described in detail by Barata et al.,[1] and only a short description will be given here. The errors in the velocities by displacement and distortion of the measuring volume due to refraction on the duct walls and change in the refractive index were found to be negligibly small and within the accuracy of the measuring equipment. Nonturbulent Doppler broadening errors due to gradients of mean velocity across the measuring volume may affect essentially the variance of the velocity fluctuations but for the present experimental conditions are on the order of $10^{-4}V_j^2$. The largest statistical (random) errors derived from populations of at least 10,000 velocity values were 0.5 and 3%, respectively, for the mean and the variance values. No corrections were made for sampling bias, but no correlations were found between Doppler frequencies and the time interval between consecutive bursts even in the zones of the flow characterized by the lowest particle arrival rates, suggesting that those effects are unimportant for the present flow conditions. Systematic errors incurred in the measurements of Reynolds shear stresses are expected to be smaller than −2.5%.

The advection and production terms in the transport equation for turbulent kinetic energy have been calculated from the results obtained in the vertical plane of symmetry and are shown in Figs. 2 and 3, normalized by V_j^3. The spatial derivatives in the k equation were obtained by second-order-accurate interpolation from 11 vertical profiles and 14 horizontal profiles covering more

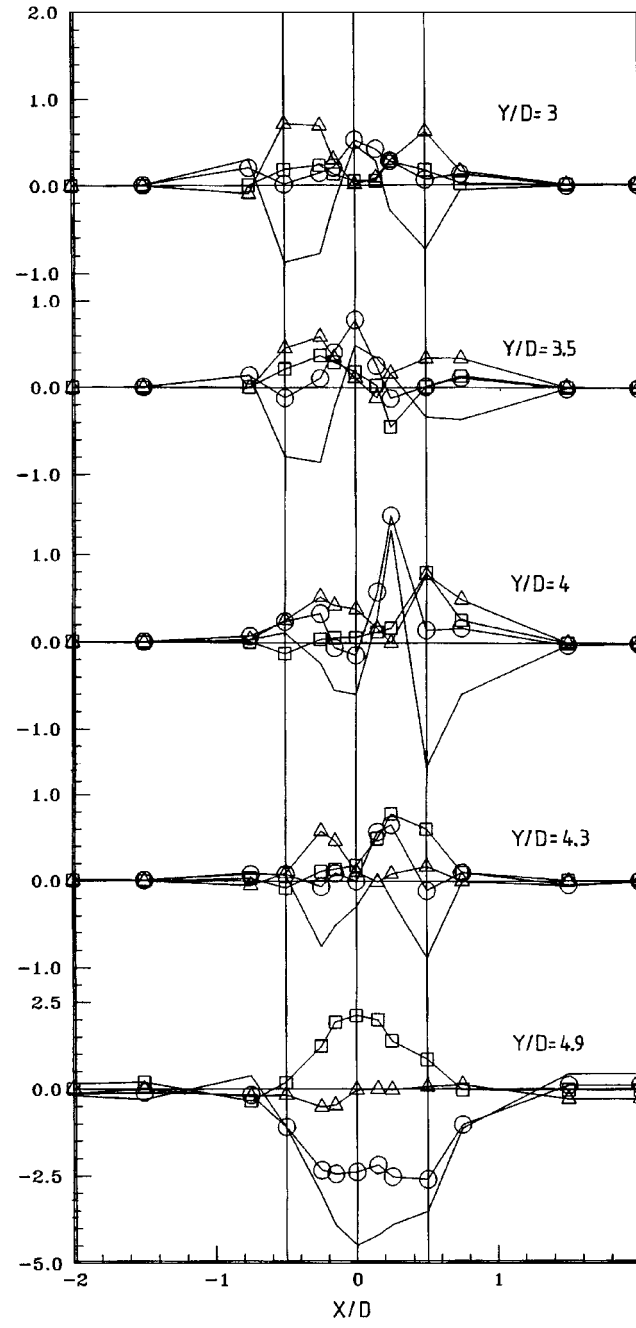

Fig. 2 Horizontal profiles of the production and convection terms in the conservation equation for turbulent kinetic energy for $Re_j = 6 \times 10^4$, H/D = 5, and V_j/U_0 = 30: ○, advection, $\bar{U}\partial k/\partial X + \bar{V}\partial k/\partial Y$; □, production by normal stresses, $\overline{u'^2}\partial\bar{U}/\partial X + \overline{v'^2}\partial\bar{V}/\partial Y$; △, production by shear stresses, $\overline{u'v'}(\partial\bar{U}/\partial Y + \partial\bar{V}/\partial X)$; and ———, imbalance (diffusion plus dissipation).

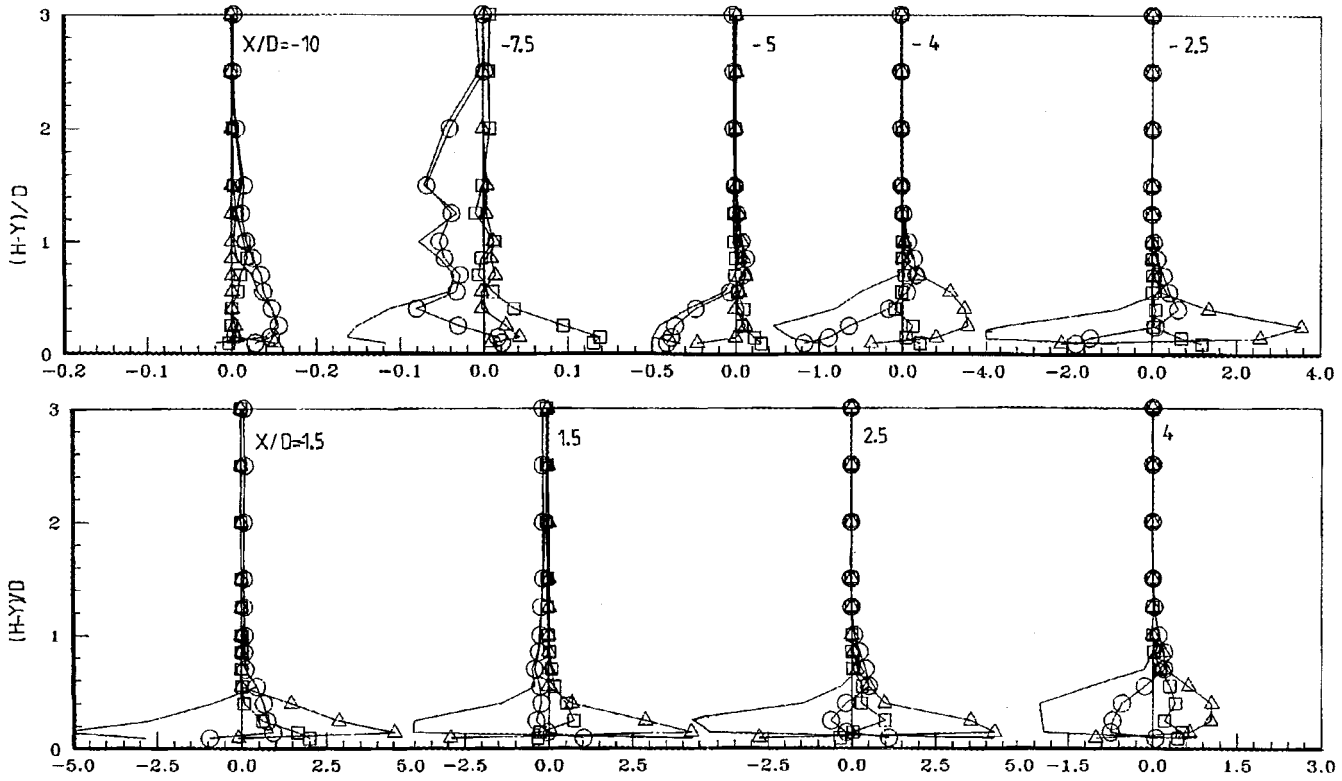

Fig. 3 Vertical profiles of the production and convection terms in the conservation equation for turbulent kinetic energy for $Re_j = 6 \times 10^4$, $H/D = 5$, and $V_j/U_0 = 30$. Symbols as in Fig. 2.

than 400 measurement stations in the region $-15 < X/D < 10$ and $0.75 < Y/D < 4.9$. The advection term was evaluated assuming that $k = 3/4(u'^2 + v'^2)$ and is plotted so that negative values represent a gain of turbulent kinetic energy. The production terms by normal and shear stresses are exact because $w'^2(\partial \bar{U}/\partial Z)$, $\overline{u'w'}$, and $\overline{u'v'}$ are equal to zero at this plane, and the positive values represent a gain of kinetic energy. The diffusive and dissipation terms were obtained by difference because they could not be measured directly, and their sign has the same meaning of the production terms.

Along the impinging jet, and particularly for $Y/D < 3.5$, the distributions of Fig. 2 resemble those for a turbulent free jet (for example, see Ref. 3) with production by shear stress as the largest term in the outer edge of the jet and likely to be balanced by turbulent dissipation. Along the center of the jet, advection is the largest term, is associated with the spread of the jet, and represents a loss of turbulent energy, which is likely to be balanced by turbulent diffusion. With the approach of the impinging zone, turbulence production is large and comparatively higher than the largest rate of production by shear stress in the impinging jet but is now predominantly through the interaction of normal stresses with normal strain and is comparable with the advection term, which represents a gain of turbulent energy. Turbulent diffusion and dissipation are expected to be large and to balance these terms. This is not surprising given the large distortion of the mean flow in the impingement zone and confirms the likely dominance of extra source terms in the balance of turbulent energy due to streamline curvature. Note that the present analysis has been referred to fixed horizontal and vertical directions similar to those used in any simple calculation scheme aimed to simulate the present flow and that a more convenient discussion may have to consider a coordinate system following a curved line as chosen by Castro and Bradshaw.[4] However, for the purpose of this Note the conclusions presented here are valid and can be used to assess the extent up to which calculation methods for thin shear layers can be extended to simulate complex impinging flows.

The relevance of the present results to the development of engineering calculation methods is that many of the principles used in current schemes for well-behaved shear layers are undermined, such as the estimation of a length scale from the shear layer thickness or the gradient-diffusion hypothesis for turbulent transport. Based on the detailed results of Castro and Bradshaw[4] for a mixing layer bounding a normally impinging plate jet with an irrotational core, one is forced toward the discussion that a further level of allowance for history effects on the distortion of turbulent flow in the impingement zone is necessary, for instance through transport equations for one or more of the empirical constants in engineering models of turbulence. This requires analysis of quantities that are not directly measurable and should involve a more detailed study of length scales in complex flows than we have been able to make in the present case.

The results of Fig. 3 show that these features of the flow are limited to the impingement zone and that the budgets of turbulent energy across the radial wall jet resemble those for a conventional wall jet (for example, see Ref. 3), with production by shear stress as the largest term and balanced by turbulent diffusion and dissipation (see, for example, the profiles at $X/D = \pm 1.5$). The deceleration of the radial jet is associated with an increase in the advection term, which represents a gain of turbulent energy and becomes comparable to the rate of production by shear stress at the same vertical station at $X/D = \pm 4$. This deceleration process is particularly important upstream of the impinging jet due to the interaction of the backward radial jet with the crossflow, and at $X/D = -5$ production of turbulent energy across the flow is almost zero and advection is the dominant term, as within other recirculating flows (for example, see Ref. 5). At $X/D = -7.5$ the approach of the stagnation point associated with the formation of the ground vortex that wraps around the impinging jet is characterized by a fast increase in the production of turbulent energy through the interaction of normal stresses with normal strains. Advection becomes small, and the distribution of Fig. 3 resembles that for wake flows. Again, the observation has important implications for the development of calculation methods because the turbulent structure of the flow in this zone is influenced by the similarity of the shear strains $\partial \bar{V}/\partial X$ and $\partial \bar{U}/\partial Y$, which precludes the use of the gradient-diffusion hypothesis for turbulent transport if the length of the ground vortex is to be predicted.

The present analysis explains in detail the reasons for the failure of the k–ε turbulence model to predict the structure of the impinging zone and the location of the ground vortex reported by Barata et al.[1] In particular, large overpredictions of the Reynolds shear stresses in

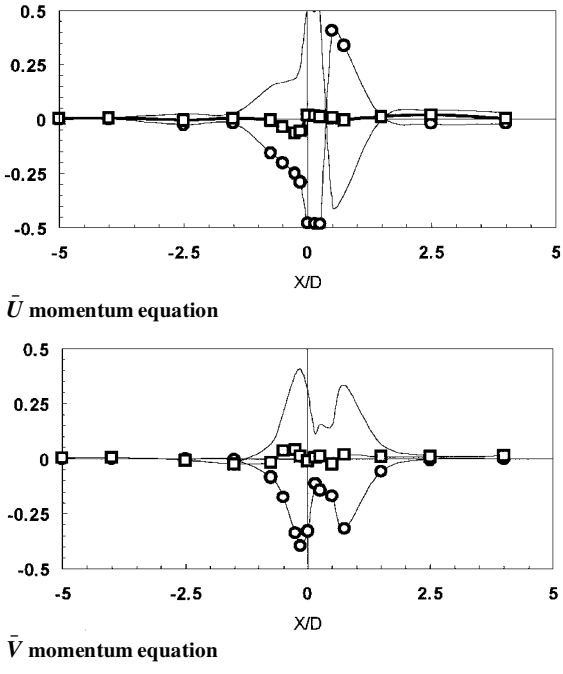

Fig. 4 Horizontal profiles of the convection (○), diffusion (□), and pressure (———) terms in the $\bar{U}$ and $\bar{V}$ momentum equations at $Y/D = 4.7$.

the impinging zone and significant regions where the sign is wrong were detected.

In spite of the failure of the k–ε turbulence model to predict the structure of the impinging zone, Barata et al.[1] also point out that the mean flow is reasonably well predicted because this type of flow is dominated by large pressure gradients. This can be explained with the help of Fig. 4, which presents the terms in the momentum equations obtained from the measurements. It shows that in the impingement region the diffusion term is negligible and the convection term is balanced by the pressure gradient term, as also observed for a low-Reynolds-number impinging jet without a crossflow (for example, see Ref. 6).

Conclusions

Budgets of turbulent kinetic energy are presented in the vicinity of the stagnation zone created by the impingement of a turbulent jet on a flat plate through a low-velocity crossflow.

Inspection of the terms in the conservation equation of the turbulent kinetic energy confirms that the turbulent structure of the flow in the ground vortex and impingement zones is associated with the interaction between normal stresses and normal strains. However, the mean flow can be reasonably well predicted using the k–ε turbulence model because the pressure gradient term in the momentum equations is dominant and is balanced by the convection term.

References

[1]Barata, J. M. M., Durão, D. F. G., Heitor, M. V., and McGuirk, J. J., "The Impingement of Single and Twin Turbulent Jets Through a Crossflow," *AIAA Journal*, Vol. 29, No. 4, 1991, pp. 595–602.

[2]Baker, O. J., "The Turbulent Horseshoe Vortex," *Journal of Wind Engineering and Industrial Aerodynamics*, Vol. 6, 1981, p. 9.

[3]Tennekees, H., and Lumley, J. L., *A First Course in Turbulence*, MIT Press, Cambridge, MA, 1972, p. 133.

[4]Castro, I. P., and Bradshaw, P., "The Structure of a Highly Curved Mixing Layer," *Journal of Fluid Mechanics*, Vol. 73, 1976, pp. 265–304.

[5]Chandrsuda, C., and Bradshaw, P., "Turbulence Structure of a Reattaching Mixing Layer," *Journal of Fluid Mechanics*, Vol. 110, 1981, pp. 171–194.

[6]Nishino, K., Samada, M., Kasuya, K., and Torii, K., "Turbulence Statistics in the Stagnation Region of an Axisymmetric Impinging Jet Flow," *International Journal of Heat and Fluid Flow*, Vol. 17, No. 3, 1996, pp. 193–201.

F. W. Chambers
Associate Editor

Mixing of Coaxial Jets with Small Annular Area in a Short Duct

S. D. Sharma* and M. R. Ahmed†
Indian Institute of Technology, Mumbai 400076, India

Nomenclature

C_p = coefficient of pressure, $(p - p_1)/0.5\rho U_m^2$
p = wall static pressure
p_1 = wall static pressure at the first station
r = radial coordinate
r_o = inner radius of the test section
U_m = mass-averaged velocity
u = streamwise mean velocity at a point
u' = rms value of streamwise velocity fluctuation
w' = rms value of transverse velocity fluctuation
x = axial (streamwise) coordinate
β = area ratio (outer to inner)
λ = velocity ratio (outer to inner)
ρ = air density
τ = nondimensional turbulence energy

Introduction

TURBULENT mixing of confined coaxial jets is a complex dynamic process that deserves a comprehensive investigation for deeper insight because it has many engineering applications. Several parameters contribute to this complexity, such as the diameter ratio of the jets, length-to-diameter ratio of the mixing duct, velocity ratio, density ratio, turbulence levels, etc. Unfortunately, information on the influence of each of these parameters still appears to be rather inadequate despite several prominent investigations that have been carried out to address the problem of the mixing of confined coaxial jets with varying conditions.[1–4] Although certain studies have contributed to the understanding of the mixing problems specific to gas turbine combustor applications with a sudden expansion[3,5] and introduction of swirl,[5–7] they have also added to the variety of the flow situation. Thus, a further widening of the scope for systematic research on the subject matter seems inevitable in view of the growing number of variables.

The present investigation deals with a particular case of mixing of coaxial jets in a nonseparating confinement with low annular-to-core-area ratio. The effect of two velocity ratios on mixing is examined for nearly a constant net mass flow rate.

Experimental Method

The experiments were carried out in a closed-circuit, all-steel wind tunnel consisting of two concentric contractions discharging airstreams with different velocities into the test section (a constant-diameter mixing duct) as shown in the inset to Fig. 1. The airflow was generated by two separate identical centrifugal blowers driven by two ac motors, each with 30-kW power. The return leg of the test rig opened into a plenum chamber that provided connections to the blower inlets. The airflow for the core stream was supplied through a settling chamber housing a perforated cone and a pair of stainless-steel wire screens serving as flow-straightening devices. Because no flow correction device was used for the annular stream, a relatively higher contraction ratio of 13.3 was employed for it against the contraction ratio of 7.4 for the core stream. The two coaxial airstreams were allowed to mix freely in the mixing duct having a length of 1000 mm and the same diameter as that of the outer jet of 380 mm. The inner jet diameter of 330 mm and its

Received Jan. 30, 1997; revision received May 27, 1998; accepted for publication June 9, 1998.

*Associate Professor, Department of Aerospace Engineering.
† Research Scholar, Department of Aerospace Engineering.